The Dependence of Electromagnetic Energy Absorption Upon Human Head Tissue Composition in the Frequency Range of 300–3000 MHz

Antonios Drossos, *Member, IEEE*, Veli Santomaa, *Senior Member, IEEE*, and Niels Kuster, *Member, IEEE*

***Abstract*—The requirements for testing compliance of cellular phones with electromagnetic safety limits demand evaluation of the maximum exposure that may occur in the user group under normal operational conditions. Under these conditions, the tissues of the ear region are most exposed, the tissue composition of which is complex and varies considerably from user to user. The objective of this paper is to derive head tissue equivalent dielectric parameters that enable the utilization of one generic homogeneous head for testing compliance for the entire user group, i.e., granting no underestimation, but also not greatly overestimating the actual maximum user exposure. As a primary study, a simple analytical model of an infinite half-space layered tissue model exposed to a plane wave was utilized to investigate the impact of impedance-matching standing waves, etc. on the spatial-peak specific absorption rate. The tissue layers were varied in composition and thickness, representing the anatomical variation of the exposed head region covering the user group including adults and children ($<$10% to $>$90% percentile). Based on the worst-case tissue layer compositions with respect to absorption at each frequency, head tissue equivalent dielectric parameters for homogeneous modeling were derived, which result in the same spatial-peak absorption. The validity of this approach for near-field exposures was demonstrated by replacing the plane wave by different near-field sources (dipoles and generic phones) and the layered structure with magnetic-resonance-image-based nonhomogeneous human head models.**

***Index Terms*—Human head modeling, mobile phones, SAR.**

I. Introduction

MOBILE telephones are RF transmitting devices that are normally operated at the user's ear. Although the time averaged output power of these devices are below 1 W, compliance with the safety limits for human electromagnetic exposure are not intrinsically granted [1].

Safety limits for electromagnetic exposures have been proposed by national and international organizations, e.g., [2], [3]. In the frequency range between 100 kHz–10 GHz, the primary dosimetric parameter for the evaluation of the exposure is the specific absorption rate (SAR). SAR is defined as the power absorbed by the unit of mass of tissue (watts/kilogram). Most regions are adopting or intend to adopt the International Commission on Non-Ionizing Radiation Protection (ICNIRP) guidelines (e.g., Europe, Japan, Korea, etc.), which define the basic limit for local exposure to be 2 W/kg averaged over a volume of 10 g and a period of 6 min [2]. The Federal Communications Commission (FCC) has adopted the slightly stricter limits of the ANSI/IEEE standard [3] for the uncontrolled environment, i.e., 1.6 W/kg averaged over a volume of 1 g and a period of 30 min.

Several standardization bodies (i.e., IEEE SCC-34 SCC-2, CENELEC TC-211 WG-2, IEC TC106, ARIB, etc.) are currently drafting recommended practices for experimental verification of compliance of mobile telecommunication devices with these basic limits. They are based on one homogeneous head model since it had previously been demonstrated that this approach is valid for the entire user group if the head shape and tissue-equivalent parameters are appropriately chosen [4], [5]. However, the scientific bases for the latter had not yet been provided.

The dielectric properties that have been used in the past for compliance testing were predetermined head tissue, such as averaged gray–white brain, gray brain, muscle tissue, etc., assuming worst-case absorption due to high losses. This does not necessarily hold true since complex absorption patterns in heterogeneous phantoms caused by impedance matching and standing waves may lead to a higher spatial-peak average SAR when compared to homogeneous modeling [5].

Absorption patterns in the human head were initially investigated on the bases of layered structures [6], [7]. The multilayered spherical model, consisting of a core of brain tissue with several additional layers of various tissues, was first investigated by Shapiro *et al.* [8] and later by Weil [9] and Kritikos and Schwan [10]. In [9], a seven-multilayered model consisting of air, skin, fat, bone, dura, cerebro spinal fluid (CSF), and brain was used, whereas in [10], a five-layered model consisting of air, skin, fat, skull, and brain was used to model the tissue structure of the head. All of the above studies focused on the absorption mechanism and resonance effects of electromagnetic (EM) energy in biological tissues when exposed to an incident plane wave and not on equivalent homogeneous worst-case simulation.

Two studies suggested homogeneous dielectric properties that overestimate the worst-case nonhomogeneous modeling. Hombach [4] investigated the dependence of EM energy

Manuscript received November 26, 1999; revised May 3, 2000.

A. Drossos and V. Santomaa are with the Nokia Research Center, FIN-00045 Helsinki, Finland.

N. Kuster is with the Swiss Federal Institute of Technology, Zurich CH-8092, Switerland.

Publisher Item Identifier S 0018-9480(00)09689-7.

TABLE I
OPERATING FREQUENCIES OF MOBILE TELECOMMUNICATION SYSTEMS

OPERATING FREQUENCY	SYSTEM
300 MHz	MPT132,
450 MHz	TETRA, NMT450, GSM450
835 MHz	AMPS
900 MHz	TACS, NMT900, GSM900
1450 MHz	PDC
1800 MHz	GSM1800
1900 MHz	PCS
2000 MHz	UMTS
2450 MHz	RLANs
3000 MHz	---

absorption on human modeling at 900 MHz using four heterogeneous phantoms based on magnetic resonance images (MRIs) with voxel sizes down to 1 mm^3. The excitation source was a half-wave dipole positioned at a distance of 15 mm from the head and with an orientation parallel to the body axis. The numerical results were compared with those of measurements in a multitissue phantom and two homogeneous phantoms of different shapes and sizes. Similarly, Meier [5] studied the dependence of EM energy absorption at 1800 MHz in the human head using the same heterogeneous phantoms as in [4] and a half-wave dipole source. Both studies derived appropriate dielectric properties of homogeneous tissue equivalent liquid for SAR compliance testing, which overestimate the worst-case heterogeneous modeling. These studies were later complemented by Schönborn *et al.* [11] investigating the difference of the absorption in children and by Burkhardt *et al.* [12] studying the appropriate modeling of the ear.

The limitations of these studies were that they only focused on the two frequency bands of 900 and 1800 MHz. In addition, they only addressed a limited variation in the layered structure of the human head and not the worst-case variation since they were based on eight randomly selected phantoms derived from MRI scans. According to Meier [5], in the frequency bands of the new generation of cellular systems, i.e., 1.5–2.5 GHz, anatomically layered structure models of the human head can lead to increased absorption in the layers due to impedance matching and standing waves, which occur in thicknesses of peripheral tissue layers in the range of $\lambda/4$–$\lambda/2$.

More comprehensive data are needed to provide a solid scientific basis for the entire user group and for a broader frequency range covering the most important bands of mobile communications between 300–3000 MHz (Table I). The objective of this paper is to derive head tissue equivalent dielectric parameters, which enable the evaluation of the compliance of mobile phones with the dosimetric safety limits for the entire user group when used under normal operational conditions, i.e., next to the ear.

II. METHODOLOGY

The tissue composition above and in the vicinity of the ear can be approximated by a layered structure consisting of cartilage, skin, fat, muscle, skull, dura, CSF, and gray and white brain matter. Since effects from impedance matching or standing waves may result in enhanced spatial-peak absorption, the worst-case tissue composition is not known *per se* and a full analysis is necessary. However, the number of combinations is too large to conduct this analysis by numerical simulations for the entire frequency range. Other more analytically based approaches had to be considered.

The authors of [1] found that the dominant absorption mechanism of biological bodies in the close near field of transmitters is inductive coupling and the absorption at the surface of the biological body can be reliably approximated based on the incident magnetic-field strengths. For the latter, the far-field consideration had only to be modified by multiplying the free-space reflection coefficient by a correction factor. However, this correction factor is only a function of the distance between the source and body with respect to the wavelength and of neither the dielectric properties nor the source. In [5], the enhancement effects observed in nonhomogeneous phantoms at 1800 MHz could be explained, verified, and analyzed by a planar layered model. In addition, the results of several studies [4], [5], [11] demonstrated that the shape of the head has only minor impact on the absorption as long as the source is operated in the closest proximity of the tissue. The combined findings of these previous studies suggest that an analytical planar model exposed by plane waves is suited as a primary study to derive worst-case tissue compositions with respect to maximum spatial-peak SAR values (maximum enhancement effects due to standing waves and impedance matching, etc.). Nevertheless, the findings must be carefully verified by near-field sources. The reason is that the field decay in the tissue may be considerably enhanced if the spatial gradient of the incident H-field normal to the surface is larger than the skin depth [1].

III. PRIMARY ANALYSES

In Fig. 1, the lateral view of facial expression muscles is presented. Four regions with major anatomical differences in tissue composition can be identified. The region of the auricularis superior muscle, the region of the occipitalis muscle, the region of the temporal bone, which is located posterior and superior to the human pinna and is free of muscle, and finally the region behind the compressed pinna. Here, adequate models of the tissue composition and thicknesses for each of these four regions have been created for young children (5–10 years old) and teenagers/adults (>10 years old). By the age of ten years, children have an almost fully developed brain with a mean weight of 1360 g [13]. According to [13], the mean weight for an adult male brain is 1400 g.

Table II shows the variations of thicknesses that are believed to cover at least the 10%–90% percentile of the user population.

The brain was homogeneously modeled as the average between gray and white matter since pronounced enhancement effects do not occur due to the brain folding. The human pinna has been rudimentarily modeled as a homogeneous layer of cartilage tissue. Notice that the thickness does not represent the actual thickness of a compressed pinna, but the minimum and maximum thickness of a homogeneous cartilage tissue that can be contained in a compressed pinna. Since the absorption in the pinna must be treated differently, the energy loss in the pinna

TABLE II
VARIATIONS OF HUMAN HEAD TISSUE THICKNESSES

Tissue	Compressed pina region		Temporal bone region		Auricularis sup. region		Occipitalis region	
	5-10y	>10y	5-10y	>10y	5-10y	>10y	5-10y	>10y
	mm	mm	mm	mm	mm	mm	mm	mm
cartil.	2-4	4-8	---	---	---	---	---	---
skin	0.5-1.5	1-2	0.5-1.5	1-2	0.5-1.5	1-2	0.5-1.5	1-2
fat	0-1	1-2	0-1	1-2	0-1	1-2	0-1	1-2
muscle	---	---	---	---	0.5-3	1-4	0.5-3	1-4
skull	1-7	1.5-7	2-7	3-7	1-7	1.5-7	2-8	3-10
dura	0.5	1	0.5	1	0.5	1	0.5	1
CSF	0-1.7	0-2	0-1.7	0-2	0-1.7	0-2	0-1.7	0-2
brain	inf.	inf.	inf.	inf.	inf.	inf.	inf.	inf.

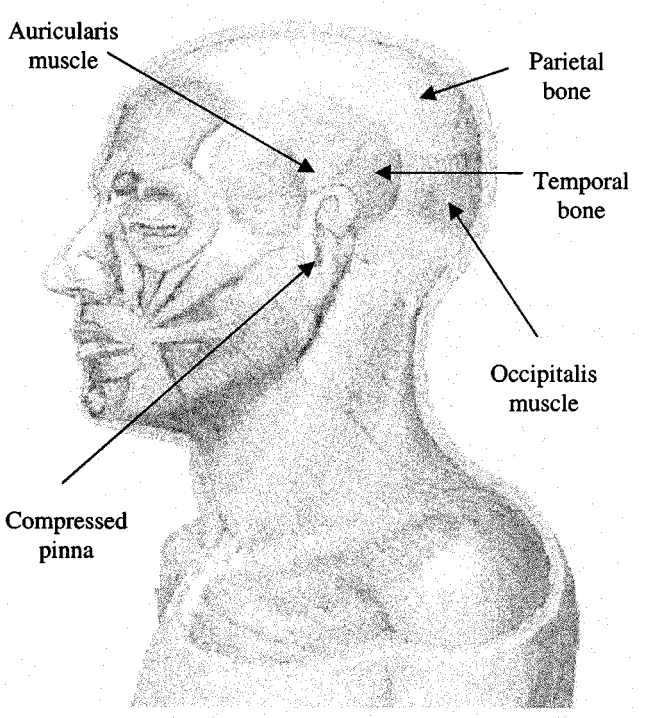

Fig. 1. Lateral view of facial expression muscles.

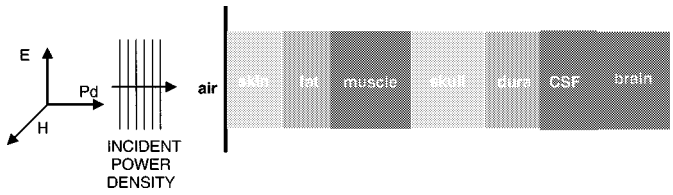

Fig. 2. Infinite half-space layered tissue models.

TABLE III
DIELECTRIC PROPERTIES AND TISSUE DENSITIES AT 900 MHz

TISSUE COMPOSITION	ε'	ε''	σ S/m	ρ kg/m^3
cartilage	42.6	15.6	0.78	1000
skin (dry/wet)	43.8	17.2	0.86	1100
fat (mean)	11.3	2.18	0.11	1100
muscle (average)	55.9	19.3	0.97	1040
skull	20.8	6.79	0.34	1850
dura	44.4	19.2	0.96	1030
CSF	68.6	48.2	2.41	1030
brain (average)	45.8	15.3	0.77	1030

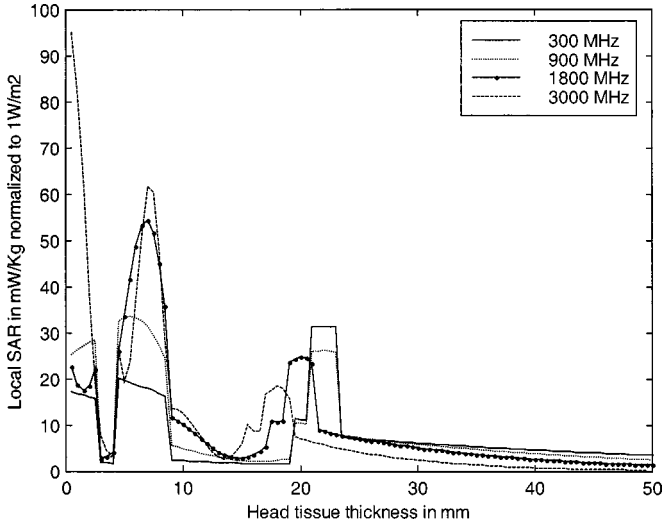

Fig. 3. Local SAR distribution for selected frequencies. Tissue combinations: 300 MHz: skin 2 mm, fat 1 mm, muscle 4 mm, skull 10 mm, dura 1 mm, CSF 2 mm, and thick brain. 900 MHz: skin 2 mm, fat 1 mm, muscle 4 mm, skull 10 mm, dura 1 mm, CSF 2 mm, and thick brain. 1800 MHz: skin 2 mm, fat 1 mm, muscle 4 mm, skull 8 mm, dura 1 mm, CSF 2 mm, and thick brain. 3000 MHz: skin 2 mm, fat 1 mm, muscle 4 mm, skull 6 mm, dura 1 mm, CSF 2 mm, and thick brain.

is not evaluated in the analysis of spatial-peak 1- and 10-g average SAR. Skin tissue consisting of epidermis and dermis has been varied here from 0.5 to 1.5 mm for children and from 1 to 2 mm for adults. This follows a reference value for the thickness of scalp skin of 1.3 mm reported in [13]. For children between 5–10 years old, the fat layer has been varied here from 0 to 1 mm and from 1 to 2 mm for ages older that ten years. The auricularis and occipitalis muscles have been varied here from 0.5 to 3 mm for children and from 1 to 4 mm for teenagers/adults. Dura tissue, consisting of the dura, subdura, and arachnoid layers, has been modeled here as 0.5- and 1-mm thick for children and teenagers/adults, respectively. In [13], the range of CSF tissue was reported between 90–150 mL under normal physiological

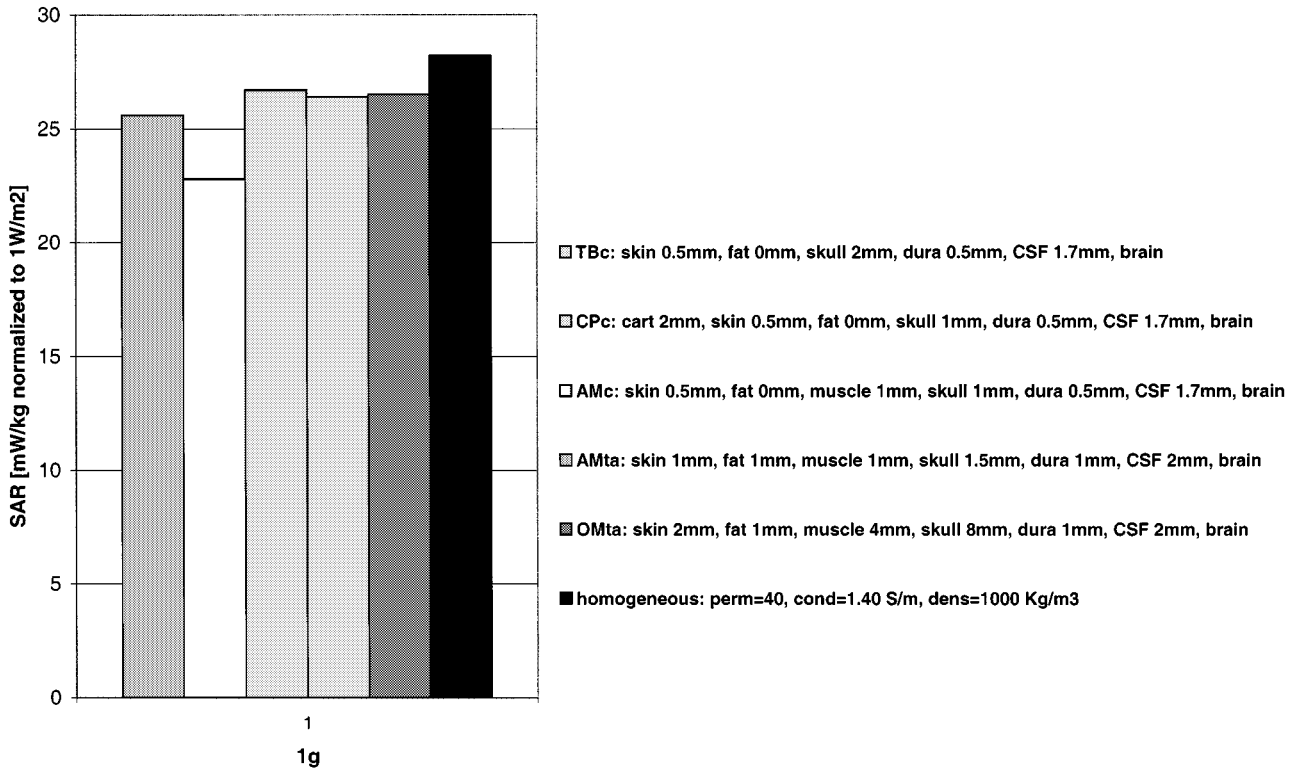

Fig. 4. Homogeneous versus nonhomogeneous modeling with respect to the spatial-peak 1-g average SAR at 1800 MHz.

TABLE IV
DIELECTRIC PROPERTIES OF HEAD EQUIVALENT TISSUES REPRESENTING WORST-CASE TISSUE COMPOSITIONS FOR 1- AND 10-g AVERAGED SPATIAL-PEAK SAR

FREQ.	ε	σ	σ
MHz		S/m	S/m
		1g	10g
300	45.3	0.87	0.70
450	43.5	0.87	0.75
835	41.5	0.90	0.80
900	41.5	0.97	0.85
1450	40.5	1.20	1.10
1800	40.0	1.40	1.40
1900	40.0	1.40	1.40
2000	40.0	1.40	1.40
2450	39.2	1.70	1.80
3000	38.5	2.10	2.40

conditions. The reference value for the CSF volume in an adult male head was reported to be 120 mL, 20% more than that of an adult female head. Assuming a spherical model for a large male adult brain with a radius of 75 mm (volume = 1767 mL), the maximum CSF layer that can surround the brain is 2 mm, corresponding to a volume of approximately 145 mL. The brain volume for five-year-old children (1300 mL [13]) is 25% less than the volume of a large adult male; consequently, the maximum thickness of the CSF layer will be 1.7 mm corresponding to a volume of approximately 105 mL. This certainly represents and overestimation from the realistic thickness of the CSF layer contained in the subarachnoid space since a considerable amount of CSF liquid is located in the brain lateral ventricles where it is formed [14]. It is apparent from Table II that the thickness of the human skull varies the most compared with that of any other tissue in the human head. This variation is accounted for by inter-individual variation, as well as for location variability (temporal and parietal bones). Temporal bone tends to be narrower in the region that is located 2 cm superior from the external auditory meatus (ear canal) [15]. The compressed pinna and auricularis muscle cover this thinnest part of the temporal bone. Here, the temporal bone thickness was modeled with a minimum of 1 mm and a maximum of 7 mm for children and with a minimum of 1.5 mm and a maximum of 7 mm for teenagers/adults for both of the regions of compressed pinna and auricularis muscle. According to [15], this represents a $<$15%–$>$85% percentile of the sample measured (5–20-year-old subjects). The temporal bone mean estimated thickness in [15] is doubled when moving superior and posterior from the external auditory meatus for both children and teenagers/adults. Thus, in the region of temporal bone identified earlier, the skull thickness was modeled with a minimum of 2 mm and a maximum of 7 mm for children and with a minimum of 3 mm and a maximum of 7 mm for teenagers/adults. The thickness of the parietal bone was measured in [16] for a sample of 96 subjects (newborn to 21 years old) at a point that is defined to be two-thirds of the way between the external auditory meatus and sagittal suture on both sides of the skull. The thickness of the parietal bone was reported for children to be between 2–8 mm and for teenagers/adults between 3–10 mm with a $<$5%–95% percentile.

The layered structures described above are irradiated by a normally incident plane wave, as shown in Fig. 2.

The generalized reflection coefficient at the section interfaces [17] was used to compute the electric fields in the medium re-

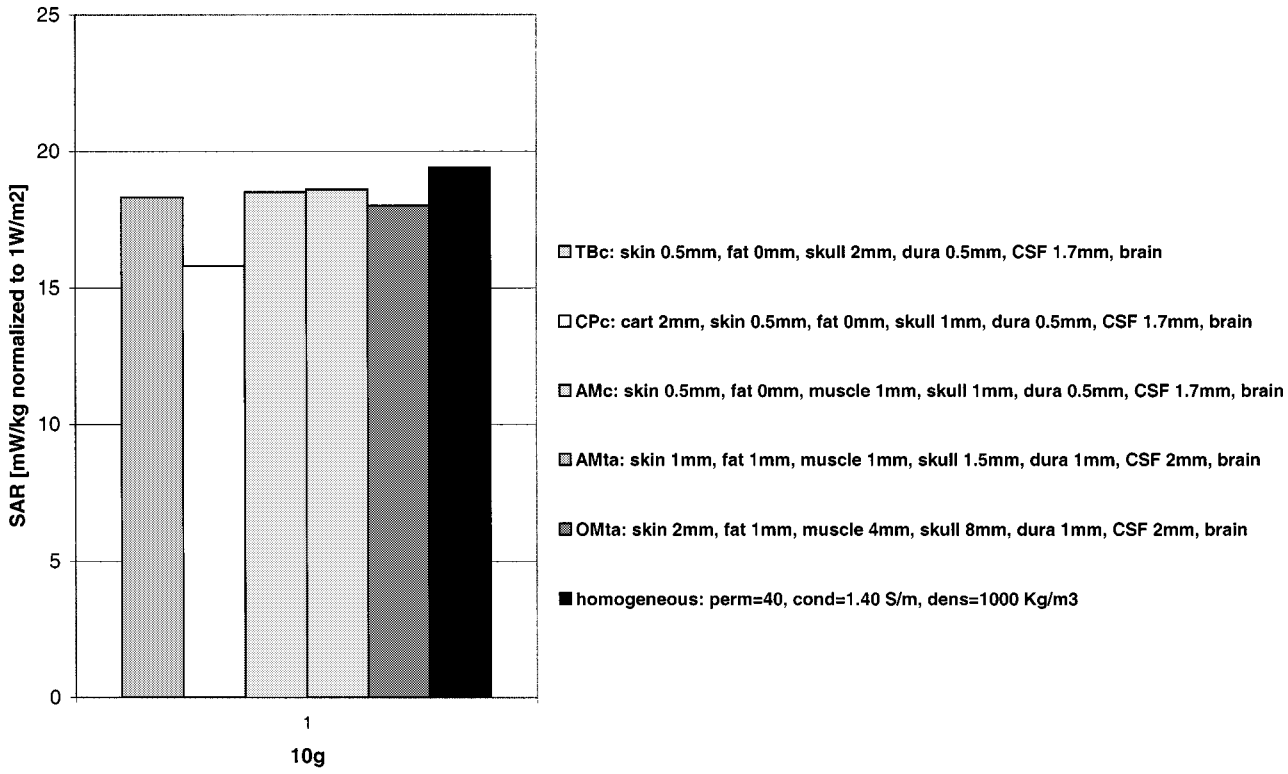

Fig. 5. Homogeneous versus nonhomogeneous modeling with respect to the spatial-peak 10-g average SAR at 1800 MHz.

cursively starting from brain tissue of infinite depth since reflections from the backside of the brain–CSF interface are negligibly small for the entire frequency range considered. The electric field values were normalized for an incident power density of $P_d = 1$ W/m^2.

The local SAR was computed with a 0.2-mm step. The spatial-peak 1- and 10-g average SARs were computed as cubic volumes with +5% tolerance in the corresponding mass. The mass-averaged spatial-peak SAR values (watts/kilograms) were derived by shifting a cube that satisfies the mass constraints over the entire region. The 1-g cubes were shifted every 0.2 mm, whereas the 10-g cubes were shifted every 0.4 mm.

The dielectric properties of the tissues used here to model the human head were computed from the 4-Cole–Cole formula [18]. In Table III, the dielectric properties and tissue densities [19] are presented for 900 MHz.

IV. Results and Discussions

A. Local SAR Distribution

Local SAR distributions for teenager/adult tissue combinations are shown in Fig. 3. These particular tissue combinations generated high spatial-peak 1-g average SAR due to a pronounced matching effect that occurs in the presence of a thick skull. The presence of the skull enhances the local SAR absorption in the peripheral skin–fat–muscle layer. Furthermore, in this particular combination, a minimum skull is incorporated in the 1-g averaging due to the maximum thickness of the peripheral layers, thus enhancing the spatial-peak 1-g average SAR. On the contrary, the spatial-peak 10-g average SAR for this combination is low due to the thick skull, which was incorporated in the 10-g averaging.

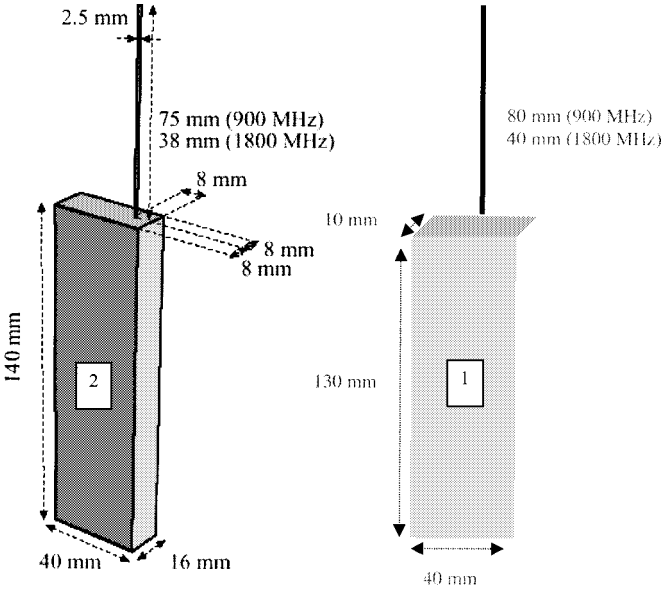

Fig. 6. Dimensions of the generic phones (quarter-wave monopoles mounted on a perfectly conducting cases).

As can be seen from Fig. 2, the absorption pattern deviates considerably as a function of frequency. As the frequency increases and the wavelength becomes shorter, standing waves occur (1800 and 3000 MHz) in the peripheral tissue layers, which have a thickness in the range of $\lambda/4$–$\lambda/2$. The 1-mm layer of fat, which follows the skin layer, causes an impedance-

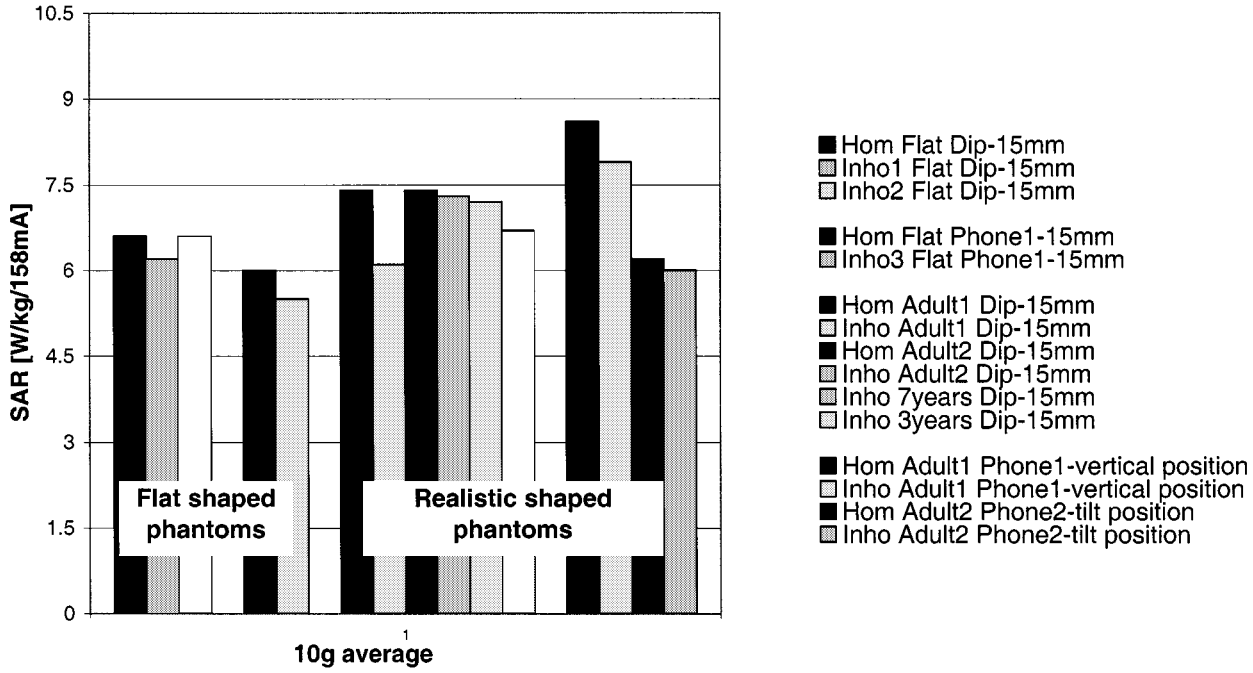

Fig. 7. Homogeneous ($\varepsilon = 41.5$, $\sigma = 0.97$ S/m, $\rho = 1000$ kg/m^3) versus nonhomogeneous modeling in the near field with respect to the spatial-peak 10-g average SAR at 900 MHz. Inho1: skin 1 mm, fat 1 mm, muscle 1 mm, skull 2 mm, dura 1 mm, CSF 2 mm, and thick brain. Inho2: skin 2 mm, fat 1 mm, muscle 4 mm, skull 2 mm, dura 1 mm, CSF 2 mm, and thick brain.

matching effect and the local SAR in the skin at 3000 MHz quadruples compared to 1800 MHz.

B. Spatial-Peak Averaged SAR

The spatial-peak 1- and 10-g averaged SAR were computed for all the tissue combinations specified in Table II and frequencies specified in Table I. A total number of 68 400 simulations were performed. For each frequency, the tissue combinations and thicknesses that result in the highest spatial-peak SAR values averaged over 1 and 10 g were evaluated. The corresponding homogeneous dielectric properties were derived by selecting the permittivity as the average of all tissues considered, whereby the conductivity was determined to result in the same (or slightly higher) spatial-peak SAR value. These equivalent tissue properties are summarized in Table IV.

The highest spatial-peak 1- and 10-g average SAR from nonhomogeneous modeling is compared to averages from homogeneous modeling at 1800 MHz in Figs. 4 and 5. The first two capital letters in the legend of Figs. 4 and 5 are abbreviation for the regions in the human head [compressed pinna: (CP), temporal bone (TB), auricularis muscle (AM), occipitalis muscle (OM)] and the following small letter stands for either children (c) or teenagers/adults (ta).

As can be seen from Figs. 4 and 5, minor differences exist in the absorption between children (5–10 years old) and teenagers/adults (>10 years old) as far as anatomical differences in tissue composition and thickness is concern. In general, the tissue composition that incorporated the maximum CSF tissue and minimum skull generated the highest spatial-peak 1- and 10-g average SAR at all frequencies under investigation. Nevertheless, the tissue composition that can be found in the occipitalis muscle region, which includes thick skull, generates very similar spatial-peak 1-g average SAR due to the impedance-matching effects and standing waves in high frequencies. This is in line with the findings of Anne [20] that the presence of the relatively low impedance of fat and bone layers may effectively transform the wave impedance of free space to that of the high lossy tissues.

As can be seen from Table IV, the conductivity for 1 g are higher than those for 10 g at the low and vice versa for the higher frequencies (2450 and 3000 MHz). This is explained by the impedance-matching effects in the peripheral tissues and the reduced wavelength. At frequencies at which all the power is absorbed within the depth of the cube, i.e., above 3 GHz, it becomes impossible to compensate the matching effects by increasing the conductivity of the homogeneous medium.

C. Comparison with Near-Field Sources

Under the premise that the worst-case tissue composition for plane-wave excitation is also appropriate for near-field sources, homogeneous modeling of planar- and MRI-based human head models with the properties in Table IV should result in higher spatial-peak SAR values than the corresponding nonhomogeneous modeling when exposed to near-field sources. This was tested at 900 and 1800 MHz by comparing the spatial-peak SAR of nonhomogeneous phantoms with the spatial peak when all tissue properties were replaced by the generic tissue of Table IV. The layered structures were first exposed to dipole sources that were orientated parallel to the layer at different distances. At the same structures, the generic phones shown in Fig. 6 were evaluated as well.

The final tests were then conducted on the bases of different MRI-based human head phantoms exposed either to a dipole source or one of the generic phones shown in Fig. 6, whereby

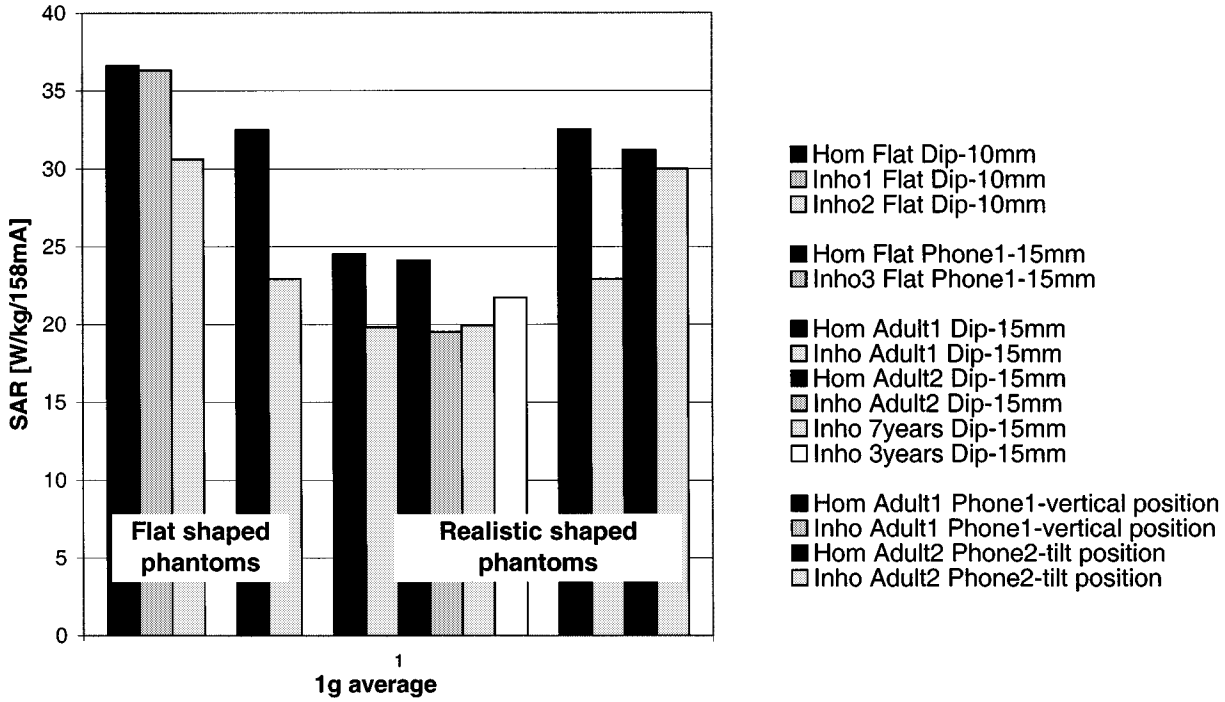

Fig. 8. Homogeneous ($\varepsilon = 40$, $\sigma = 1.4$ S/m, $\rho = 1000$ kg/m^3) versus nonhomogeneous modeling in the near field with respect to the spatial-peak 1-g average SAR at 1800 MHz (for composition of Inho1 and Inho2, see Fig. 7).

the distances as well as the orientations were varied. The head phantom Adult1 corresponded to the phantom head available from the Remcom Corporation, State College, PA. The other head phantoms are described in [4], [5] and [11], [12]. The computations were conducted with finite-difference time-domain algorithms (XFDTD by Recom Corporation, State College, PA and SEMCAD by Schmid & Partner Engineering AG, Zurich, Switzerland).

The spatial-peak SAR values obtained with the homogeneous modeling were always larger than those from nonhomogeneous modeling. In Figs. 7 and 8, a selection of these results are summarized, which demonstrated the validity of the approach chosen in this paper. However, slight underestimation of the 10-g averaged values may theoretically occur at 3 GHz under worst-case conditions, e.g., with the worst-case layer composition and when the source is within less than a few millimeters from the tissue. The reason is that, under these conditions, all the power is absorbed within the averaging cube such that the larger conductivity does not compensate for the matching effects.

V. Conclusions

The effects of the head tissue variability in the ear area on the spatial-peak SAR values averaged over 1 and 10 g have been analyzed for the frequency range of 300–3000 MHz. Based on this analysis, head tissue equivalent dielectric properties for homogeneous media have been derived that appropriately simulate the maximum absorption of the worst-case tissue composition. Using these dielectric properties in combination with the worst-case head shape will enable scientifically sound compliance testing of mobile telecommunication equipment, which are operated next to the ear. Such testing will be conservative in the sense that it will ensure that the exposure is not underestimated for a considerable cross section of the user population (<10%–>90% percentile). Hence, this paper closes an important scientific gap for finalizing reliable and sound compliance testing procedures.

Acknowledgment

The authors gratefully acknowledge the advice of T. Schmid, Schmid & Partner Engineering AG, Zurich, Switzerland, and A. Toropainen, Nokia Research Center, Helsinki, Finland, as well as the help of A. Brehonnet, Nokia Research Center, Helsinki, Finland.

References

[1] N. Kuster and Q. Balzano, "Energy absorption mechanism by biological bodies in the near field of dipole antennas above 300 MHz," *IEEE Trans. Veh. Technol.*, vol. 41, pp. 17–23, Feb. 1992.

[2] International Commission on Non-Ionizing Radiation Protection, "Health issues related to the use of hand-held radiotelephones and base transmitters," *Health Phys.*, vol. 70, pp. 587–593, 1996.

[3] *IEEE Standard for Safety Levels with Respect to Human Exposure to Radio Frequency Electromagnetic Fields, 3 kHz to 300 GHz*, ANSI/IEEE Standard C95.1-1992, 1992.

[4] V. Hombach, K. Meier, M. Burkhardt, E. Kuhn, and N. Kuster, "The dependence of EM energy absorption upon human head modeling at 900 MHz," *IEEE Trans. Microwave Theory Tech.*, vol. 44, pp. 1865–1873, Oct. 1996.

[5] K. Meier, V. Hombach, R. Kästle, R. Y. S. Tay, and N. Kuster, "The dependence of EM energy absorption upon human head modeling at 1800 MHz," *IEEE Trans. Microwave Theory Tech.*, vol. 45, pp. 2058–2062, Nov. 1997.

[6] H. P. Schwan and K. Li, "Hazards due to total body irradiation," *Proc. IRE*, vol. 44, pp. 1572–1581, Nov. 1956.

[7] D. E. Livesay and K. M. Chen, "Electromagnetic fields induced inside of biological bodies," in *IEEE S-MTT Int. Microwave Symp. Dig.*, Atlanta, GA, 1974, pp. 35–37.

[8] A. R. Shapiro, R. F. Lutomirski, and H. T. Yura, "Induced heating within a cranial structure irradiated by an electromagnetic plane wave," *IEEE Trans. Microwave Theory Tech.*, vol. MTT-19, pp. 187–196, Feb. 1971.
[9] C. M. Weil, "Absorption characteristics of multilayered sphere models exposed to UHF/Microwave radiation," *IEEE Trans. Biomed. Eng.*, vol. BME-22, pp. 468–476, Nov. 1975.
[10] H. N. Kritikos and H. P. Schwan, "Formation of hot spots in multilayered spheres," *IEEE Trans. Biomed. Eng.*, vol. BME-22, pp. 168–172, Mar. 1976.
[11] F. Schönborn, M. Burkhardt, and N. Kuster, "Differences in energy absorption between heads of adults and children in the near field of sources," *Health Phys.*, vol. 74, no. 2, pp. 160–168, Feb. 1998.
[12] M. Burkhardt and N. Kuster, "Appropriate modeling of the ear for compliance testing of handheld MTE with SAR safety limits at 900/1800 MHz," *IEEE Trans. Microwave Theory Tech.*, to be published.
[13] Int. Commission Radiol. Protection, *Report of the Task Group on Reference Man*. New York: Pergamon, 1975.
[14] E. Gardner, D. J. Gray, and R. O. Rahilly, *Anatomy*, 2nd ed. Philadelphia, PA: Saunders, 1963.
[15] D. L. Simms and J. G. Neely, "Thickness of the lateral surface of the temporal bone in children," *Annu. Otol. Rhinol. Laryngol.*, vol. 98, pp. 726–731, 1989.
[16] W. J. Koenig, J. M. Donovan, and J. M. Pensler, "Cranial bone grafting in children," *Plastic Reconstructive Surgery*, vol. 95, pp. 1–4, Jan. 1995.
[17] W. C. Chew, *Waves and Fields in Inhomogeneous Media*. Piscataway, NJ: IEEE Press, 1995, pp. 45–53.
[18] Microwave Consultants, *Dielectric Database*. London, U.K.: Microwave Consultants Ltd., 1994.
[19] M. A. Jensen and Y. Rahmat-Samii, "EM interaction of handset antennas and a human in personal communications," *Proc. IEEE*, vol. 83, pp. 7–17, Jan. 1995.
[20] A. Anne, "Scattering and absorption of microwaves by dissipative dielectric objects: The biological significance and hazards to mankind," Ph.D. dissertation, Dept. Elect. Eng., Univ. Pennsylvania, Philadelphia, PA, July, 1963.

Antonios Drossos (M'00) was born in Rhodos, Greece, in October 1973. He received the B.Sc. degree in electronics from the Technical Institute of Iraklio, Iraklio, Greece, and the M.Sc. degree in electrical engineering from the Tampere University of Technology, Tampere, Finland, and is currently working toward the Ph.D. degree at the Tampere University of Technology.

In 1998, he join the Nokia Research Center, Helsinki, Finland, where he has been involved in SAR dosimetry research. He has authored or co-authored papers in journals and conferences.

Veli Santomaa (S'68–M'69–SM'89) received the M.S.E.E. and Licentiate in Technology degrees from the Helsinki University of Technology, Espoo, Finland, in 1986 and 1963, respectively.

From 1962 to 1994, he was with the Technical Research Center of Finland (VTT). From 1974 to 1983, he was the Head of the Radio Department and from 1983 to 1993, the Director of the Telecommunications Laboratory. In 1994, he joined the Nokia Research Center, Helsinki, Finland, as a Principal Scientist, where his responsibilities are in the field of electromotive force (EMF) and antennas, participating in the standardization, international industry cooperation, chairing the Nokia-wide EMR Working Group, and conducting research in the field. As a secondary occupation, from 1964 to 1969, he was an Assistant in Electronics and Electrical Engineering, Helsinki University of Technology. From 1969 to 1981, he has been a Lecturer of electronics and electrical engineering. From 1979 to 1997, he was a Lecturer of radio technology at the Military Academy of Finland. He has been responsible for many research and development projects on radio-wave propagation, radio network planning, radio links and other radio systems, satellite communication, satellite television receiving equipments, antennas (especially radar antennas), and microwave components. He has authored or co-authored numerous papers in these fields.

Prof. Santomaa has been chair of the Electronics Section of the Scientific Committee of National Defence from 1994 to 1997 and, since 1998, has been a member of the Committee and chair of the Information Technology Section.

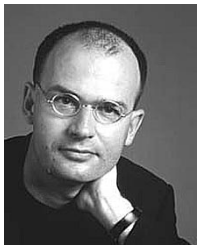

Niels Kuster (M'93) was born in Olten, Switzerland, in June 1957. He received the Diploma and Ph.D. degrees in electrical engineering from the Swiss Federal Institute of Technology (ETH), Zurich, Switzerland.

In 1985, he joined the Electromagnetics Laboratory, ETH, where he was involved in the research and development of the generalized multipole technique (GMT) and the three-dimensional (3-D) multiple multipole program (MMP) code. In 1992, he was an Invited Professor at Motorola Inc., Fort Lauderdale, FL, for a trimester. He is currently a Professor in Department of Electrical Engineering, ETH, and the Designated Director of the Foundation for Research on Information Technologies in Society (IT'IS), Zurich, Switzerland. His research interests include all aspects of numerical techniques in electrodynamics, near-field measurement techniques, antenna design, and the biological effects of electromagnetic fields.

Dr. Kuster is a member of various scientific societies and URSI Commission K.